

Attosecond Pump Probe: Exploring Ultrafast Electron Motion inside an Atom

S. X. Hu* and L. A. Collins†

Theoretical Division, Los Alamos National Laboratory, Los Alamos, New Mexico 87545, USA

(Received 28 November 2005; published 24 February 2006)

The attosecond pump probe, in close analogy to the standard femtosecond probing technique, has been proposed and theoretically demonstrated with its application to explore ultrafast electron motions inside atoms. We have performed realistic modeling for the full dynamics of both the femtosecond pumping and the attosecond probing processes. Our simulations have illustrated that an ultrashort oscillation period of 2.0 fs can be mapped out for a wave packet in low-lying excited states of the helium atom. This opens the prospect of a wealth of similar pump probe experiments to examine ultrafast electronic or atomic motions.

DOI: [10.1103/PhysRevLett.96.073004](https://doi.org/10.1103/PhysRevLett.96.073004)

PACS numbers: 32.80.Fb, 32.80.Rm, 42.65.Re

Dynamical motion of atoms within molecules and solids can be captured with pump probe techniques using ultrashort laser pulses [1–3] as witnessed by observations of the evolution of a chemical reaction [4] or the melting of a solid *in situ* [5]. The exploration of even faster processes, such as electron motion inside an atom, has now become possible with the generation of attosecond (as = 10^{-18} s) extreme ultraviolet (EUV) pulses [6–8]. This has stimulated experiments on the Auger decay dynamics of atoms [9] and the control of above-threshold ionization [10] with, however, the attosecond pulse employed mainly as a pumping tool. In this Letter, we theoretically demonstrate that an attosecond pulse also can effectively *probe* the extremely fast motion of an electronic wave packet in an atom. Pumped by a broadband femtosecond UV pulse, one electron of ground-state helium can be launched into a superposition of low-lying excited states, thus forming a wave packet that begins to oscillate relative to the atomic core. A time-delayed attosecond EUV pulse (probe) then ionizes the atom causing three-body breakup. Measuring either the energy sharing of the ionized electrons or the total ionization probability as a function of the time delay determines the correlation (overlap) of the electrons at the instant of the probe. Since this correlation depends on the separation of the two electrons, following one of these quantities in time displays the internal motion of the excited electron. Our simulation has demonstrated that an ultrashort oscillation period of 2 fs can be followed for several cycles.

An attosecond pump-probe experiment has a close analogy to the standard femtosecond technique used in chemistry and solid-state physics, namely, the initiation of dynamics in a system by a pump pulse and the observation of the temporal evolution of this system with a time-delayed probe pulse. These time-delayed measurements can, in principle, trace out extremely fast dynamics. For example, we can explore with an attosecond pump-probe mechanism the motion of an electron wave packet inside an atom. To theoretically demonstrate this technique, we show its basic features in the schematic diagram Fig. 1. We consider a ground-state helium (He) atom, a prototypical

two-electron system, pumped first by a femtosecond UV pulse as indicated by the left panel of Fig. 1. Such a pulse interaction can launch one of the two ground-state electrons ($1s^2$) into $1snp$ states of He ($n = 2, 3, 4, \dots$) due to the broad bandwidth of the UV pulse (middle panel of Fig. 1). After the pump stage, the excited electron wave packet periodically oscillates between the nuclear core and its outer turning point while the inner electron remains close to the nucleus. Since the Coulomb correlation between the two electrons mainly depends on their relative separation, we expect dynamical electron correlation between the inner and the outer electrons. Such dynamical correlation can be captured by an ultrashort attosecond pulse. For instance, applying an attosecond EUV pulse to the pumped system at a time at which the outer electron attains a large separation from the nucleus will result in the core electron absorbing most of the EUV photon energy, thereby leaving the atom quickly. The outer electron experiences a suddenly changed potential and subsequently ionizes, the so-called “shake-off” process [11–13]. The two electrons so ejected have an asymmetric energy sharing, illustrated in the upper diagram of the right panel of Fig. 1. On the other hand, if the attosecond probe occurs when the outer-electron wave packet comes closest to the core, the two strongly correlated electrons will most proba-

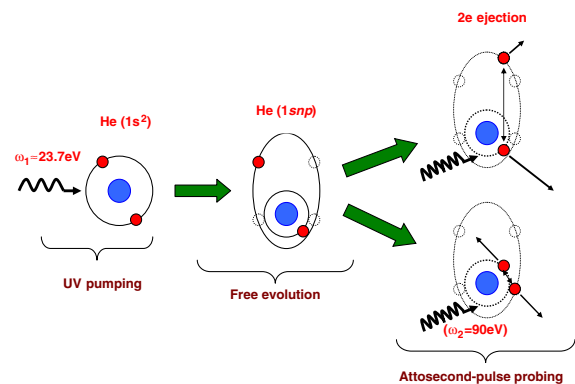


FIG. 1 (color online). Schematic diagram of the attosecond pump probe.

bly share the EUV photon energy and will both be “knocked out” from the atom [14–16], as shown in the lower diagram. Thus, by varying the time delay between the pump and the attosecond probe, we expect to map out the electron correlation by measuring the energy sharing between the two ejected electrons. Consequently, we can directly follow the dynamical motion of the “target” electron wave packet. Furthermore, as we shall show below, the total probability for double ionization in such an attosecond pump-probe scheme will also depend on the electron correlation, and so on the time delay τ .

The fully six-dimensional (6D) time-dependent Schrödinger equation, which governs the interaction dynamics of such a two-electron system with external fields, has the following form (atomic units are used throughout):

$$i \frac{\partial}{\partial t} \Phi(\mathbf{r}_1, \mathbf{r}_2|t) = \left[-\frac{1}{2}(\Delta_{\mathbf{r}_1} + \Delta_{\mathbf{r}_2}) - \frac{2}{r_1} - \frac{2}{r_2} + \frac{1}{|\mathbf{r}_1 - \mathbf{r}_2|} + \mathbf{E}(t) \cdot (\mathbf{r}_1 + \mathbf{r}_2) \right] \Phi(\mathbf{r}_1, \mathbf{r}_2|t), \quad (1)$$

where \mathbf{r}_1 and \mathbf{r}_2 are the position vectors of each electron, with respect to the nucleus. The UV/EUV pulse interaction is expressed by the last term in the above equation. We obtain a more tractable solution by following the time-dependent close-coupling recipe [17–19]: expanding the 6D wave function $\Phi(\mathbf{r}_1, \mathbf{r}_2|t)$ in terms of bipolar spherical harmonics $\mathcal{Y}_{l_1 l_2}^{L,M}(\Omega_1, \Omega_2)$, $\Phi(\mathbf{r}_1, \mathbf{r}_2|t) = \sum_{LM} \sum_{l_1 l_2} \times \frac{\Psi_{l_1 l_2}^{(LM)}(r_1, r_2|t)}{r_1 r_2} \mathcal{Y}_{l_1 l_2}^{L,M}(\Omega_1, \Omega_2)$, for a specific symmetry (LM). Also, we can expand the Coulomb repulsion term $1/|\mathbf{r}_1 - \mathbf{r}_2|$ and the field interaction $\mathbf{E}(t) \cdot (\mathbf{r}_1 + \mathbf{r}_2)$ in terms of spherical harmonics. Substituting these expansions into the above Schrödinger equation (1) and integrating over the angles Ω_1 and Ω_2 yields a set of coupled partial differential equations with only two radial variables r_1 and r_2 :

$$i \frac{\partial}{\partial t} \Psi_j(r_1, r_2|t) = [\hat{T}_1 + \hat{T}_2 + \hat{V}_c] \Psi_j(r_1, r_2|t) + \sum_k \hat{V}_{j,k}^I(r_1, r_2|t) \Psi_k(r_1, r_2|t), \quad (2)$$

where the partial wave index j runs from 1 to the total number N of partial waves used for expansion. In such a referencing scheme, each index j corresponds to a specific momentum combination (L, M, l_1, l_2). In Eq. (2), the diagonal operators \hat{T}_1, \hat{T}_2 , and \hat{V}_c give the kinetic energies and the Coulomb attractions between each electron and the nucleus, while the off-diagonal potential term $\hat{V}_{j,k}^I(r_1, r_2|t)$ consists of the Coulomb repulsion between two electrons and their interactions with external fields. Since both the pump and the probe pulses are linearly polarized, we may set the magnetic quantum number to zero in the case of ground-state He ($M = 0$) atom targets.

Combining the real-space-product algorithm with the fine-gridding scheme of the finite-element discrete-

variable representation [20], we have numerically solved the coupled equations (2). First, we relaxed a trial wave packet with six partial waves ($l_1 = l_2 = 0-5$ and $L = 0$) in imaginary time and obtained a ground-state energy of -2.9031 a.u., in excellent agreement with the experimental value of -2.9037 a.u. for He. In our subsequent calculations for the pump-probe dynamics, we have employed a total of 34 partial waves in the expansion of which the total angular momentum L varies from 0 to 3, including all possible combinations with $l_1 = l_2 = 0-5$ in the case of $L = 0$, and $l_1 = l_2 = 0-4$ for $L \neq 0$. We have checked the convergence by adding additional partial waves in the expansion and found little sensitivity. The two-dimensional grids used here extend out to ~ 235 Bohr radii, spanned by 220 finite elements. In addition, we enforced an absorption edge for large r_1 and r_2 boundaries to avoid wave reflections from the “walls.”

We initiate a pump UV pulse to interact with the ground-state He atom [indicated in Fig. 2(a) at $t = 0$]. The UV pulse has a peak intensity of $I_1 = 6 \times 10^{14}$ W/cm², a duration (T_1) of 1.5 fs, and a broad bandwidth of $\Delta\omega_1 \approx 4.0$ eV (FWHM of its frequency spectrum) around its central frequency of $\omega_1 \approx 23.7$ eV. The frequencies contained within this bandwidth can excite all $1snp$ states for $n = 2, 3, 4, \dots$ with some portion even in the continuum. The excitation probability is equal to $\sim 54\%$ for the pumping pulse parameters concerned. At the end of the interaction ($t = 1.5$ fs), a bound electron wave packet forms,

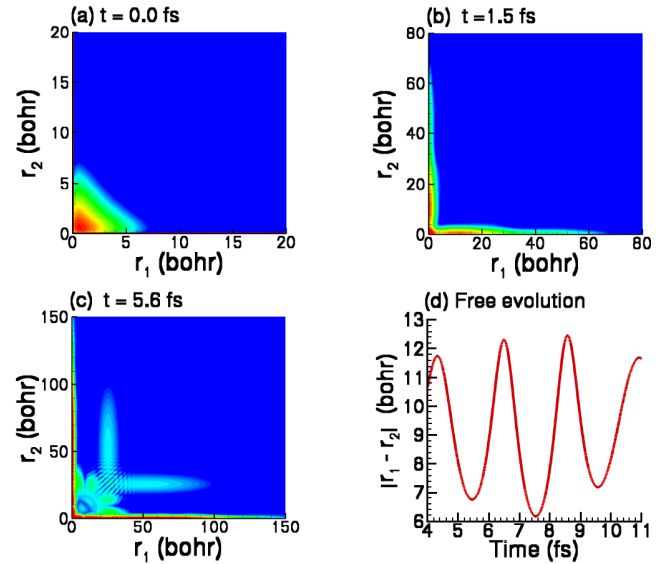


FIG. 2 (color online). Snapshots of electron probability distribution on the (r_1, r_2) plane for different instants: (a) The initial ground state of He; (b) at the end of the UV pumping; (c) at $t = 5.6$ fs, that is, after the 250 as probe pulse starting at $\tau = 5.1$ fs, and freely propagating for another 250 as after the as-pulse passes. (d) The normalized interelectron distance $|\mathbf{r}_1 - \mathbf{r}_2|$ as a function of time, for the free evolution (without probing) of the pumped He.

which is illustrated by Fig. 2(b) that plots the electron probability ($\sum_j |\Psi_j(r_1, r_2|t)|^2$ for all j) against r_1 and r_2 . The probabilities are large along the two axes indicating that one electron is near zero while the other is at a substantial distance from the nucleus, which illustrates the excitation of a *single* electron. The analysis of the probability distribution further confirms excitation mainly to (*sp*) and (*ps*) partial waves with $L = 1$, through the single-photon excitation channel. After the pumping pulse passed, the excited electron wave packet does a “breathing” motion (back and forth oscillation) relative to the core electron. As one expects, the expectation value of interelectron distance $|\mathbf{r}_1 - \mathbf{r}_2|$ exhibits an oscillation for the free evolution of the pumped He, which is indicated in Fig. 2(d). With attosecond probes one can map this oscillation by measuring the double-ionization cross sections.

After having the pumped He freely evolve for a few femtoseconds (in order for any pump-induced ionizing wave packets to leave the calculation box), we start to probe the bound wave packet motion from $t = 4.0$ fs by shining an attosecond EUV pulse on the pumped system. The applied pulse has a duration of 250 as, a peak intensity of $I_2 = 3 \times 10^{15}$ W/cm² (making substantial double-ionization probability), a photon energy of $\omega_2 = 90$ eV, and a \sin^2 envelope. After the time-delayed attosecond pulse strikes, we normally allow the system to relax freely for another ~ 250 as, permitting a more accurate determination of the ionization cross sections. As an example, we show in Fig. 2(c) the electron probability (for all partial waves) distribution at $t = 5.6$ fs for the 250 as probe pulse turning on at $\tau = 5.1$ fs. Since a single EUV photon can break apart the excited He atom, we observed electron probabilities in both large r_1 and large r_2 regions, indicating the simultaneous ejection of both electrons (i.e., the $2e$ -ejection process). As we discussed above, the probe pulse is so short that the electron correlation information is instantly frozen and captured at the breaking up of the three-body Coulomb system. Therefore, by measuring the cross sections for $2e$ ejection, we may obtain the dynamical information on the electron wave packet motion.

In essence, the attosecond pump probe process induces $2e$ ejection of He by the successive absorption of two photons—one UV photon excitation and one EUV photon probing. To evaluate the pump-probe-induced double-ionization cross sections, we first project the normalized double continuum of He²⁺ onto the total wave function [19] at the end of probe process. From the resulting double-ionization wave function ($L = 0, 2$) in momentum space, we can then compute the total and the triple-differential (TDCS) cross sections [19]. Although the probing photon ($\omega_2 = 90$ eV) can also cause double ionization of the unpumped ground-state He, these solely probe-induced ionization waves ($L = 1$) can be excluded from our calculations of pump-probe-induced ($L = 0, 2$) double-ionization cross sections. Essentially, these two processes

result in *different* total energies for the two ejected electrons, which may be distinguished in coincident experiment measurements. The calculated results are illustrated for various time-delayed attosecond probes in Figs. 3 and 4. In Fig. 3(a), we display the total cross section for the pump-probe-induced $2e$ ejection as a function of the time delay τ between the pump and the initiation of the probe pulse. We clearly find that the total cross section periodically oscillates in τ . When the attosecond probe occurs at the instant that the outer-electron wave packet approaches the inner one [for example, at $t \approx 5.5$ fs in Fig. 2(d)], strong correlation facilitates the ionization of the two electrons, thereby resulting in a peak in the total cross section for double ionization. On the other hand, if the electron wave packet is located at its outer turning point during the attosecond probe [e.g., at $t \approx 6.5$ fs in Fig. 2(d)], then a minimum in the double-ionization cross section will occur. Thus, the oscillation cycle of ~ 2.0 fs in Fig. 3(a) is just a measure of the breathing motion period for the electron wave packet.

Calculating the triple-differential cross sections of the $2e$ -ejection process for different time delays in attosecond pump probes further confirms this observation. The coplanar (i.e., $\phi_1 = \phi_2 = 0$) results are shown by Fig. 4 in which we display the TDCS as a function of the second electron energy (E_2) and its ejection angle θ_2 , while fixing the first electron ejection angle at $\theta_1 = 90^\circ$ with respect to the pulse polarization axis. The two electrons share the total energy of the pump and probe photons. We show eight panels in Fig. 4 for different time delays τ . In these contour plots, red represents the maximum value and blue, the minimum TDCS. For all panels, we present the “back-to-back” ejection configuration, which best captures the electron repulsion by observing the second electron ejecting at around $\theta_2 = 270^\circ$. With this configuration considered, we can avoid “contaminations” of single ionization (mainly along the pulse polarization axis, i.e., $\theta = 0^\circ$) to our TDCS calculations. For various time delays τ , we clearly observe different features of energy sharing be-

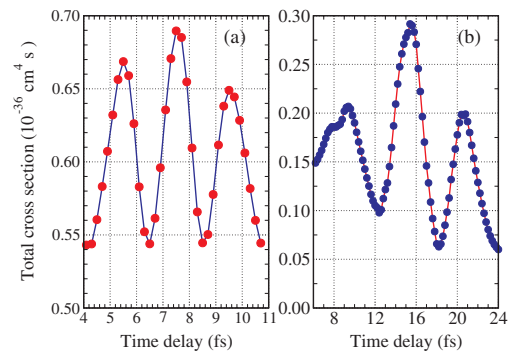


FIG. 3 (color online). The total cross section for double ionization of He vs the time delay between pump and probe pulses, for situations of different pumping UV pulses with durations: (a) $T_1 = 1.5$ fs and (b) $T_1 = 6.0$ fs.

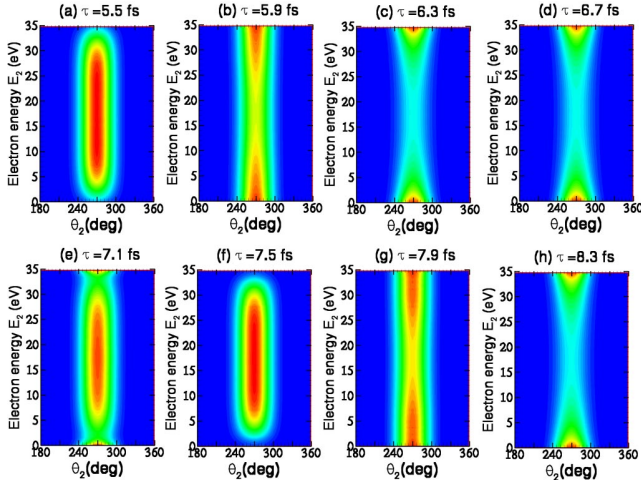


FIG. 4 (color online). The contour plots for triple-differential cross sections of He double ionization under the attosecond pump probe scheme, for the case of the pumping pulse $T_1 = 1.5$ fs in Fig. 3(a).

tween the two ejected electrons. For example, at $\tau = 5.5$ fs [indicated by Fig. 4(a)] we find that the TDCS has a “flat-top” maximum in the energy range of 10 ~ 25 eV. This indicates that the two ejected electrons tend to share the EUV photon energy symmetrically, which illustrates the knockout mechanism as being recently confirmed in experiments [21]. When τ increases to 5.9 fs, the energy sharing among two electrons starts to become asymmetric, as shown by Fig. 4(b). If the time delay τ is further increased, we find that the electron energy sharing becomes more and more asymmetric as in Figs. 4(c) and 4(d). For these latter cases, one electron takes most of the excess photon energy and leaves the atom quickly while the other electron shakes off at a much slower velocity. This corresponds to the situation in which the two electrons are well separated at the instant of probing. However, by further delaying the probe pulse, a symmetric energy sharing, similar to what we have seen at $\tau = 5.5$ fs, reappears at $\tau = 7.5$ fs as illustrated by Fig. 4(f). This signals the return of the electron wave packet to the vicinity of the nucleus. Similar energy-sharing features repeat themselves periodically with increasing τ . The period of ~ 2.0 fs is the same as seen in the total cross section [Fig. 3(a)]. In fact, the occurrence of symmetric energy sharing in TDCS is exactly coincident with the appearance of the peak in the total cross section and of the minimum in $|\mathbf{r}_1 - \mathbf{r}_2|$ [Fig. 2(d)]. In addition to the short pumping case of $T_1 = 1.5$ fs discussed above, we have also investigated the situation for a longer ($T_1 = 6.0$ fs) UV pump pulse for which all other parameters remain the same. Its bandwidth becomes narrower ($\Delta\omega_1 \sim 1$ eV) and covers only the $1snp$ states with $n = 3, 4, 5, \dots$. This means that the created

electron wave packet may move slower, since the fast $1s2p$ component (its oscillation period $t_K = 2\pi n^{*3}$ a.u. ~ 1.17 fs [22]) is now excluded. The attosecond pump probe results are plotted in Fig. 3(b) from which a breathing motion period of ~ 5.8 fs can be inferred.

In this Letter, we have theoretically demonstrated the attosecond pump probe technique with its application to probing ultrafast electron motion in low-excited states of an atom. Through feasible measurements of double-ionization cross sections, we can directly trace out the rapid electron wave packet motion inside an atom in time. Such a technique may find numerous important applications for exploring ultrafast dynamics in nature, such as, atomic core excitations and ultrafast molecular imaging.

Work performed under the auspices of the U.S. Department of Energy through the Los Alamos National Laboratory.

*Electronic address: suxing@lanl.gov

†Electronic address: lac@lanl.gov

- [1] S. Woutersen and H. J. Bakker, *Nature (London)* **402**, 507 (1999).
- [2] S. M. Hurley *et al.*, *Science* **298**, 202 (2002).
- [3] T. V. Truong, L. Xu, Y. R. Shen, *Phys. Rev. Lett.* **90**, 193902 (2003).
- [4] H. Ihee *et al.*, *Science* **291**, 458 (2001).
- [5] A. M. Lindenberg *et al.*, *Science* **308**, 392 (2005).
- [6] M. Drescher *et al.*, *Science* **291**, 1923 (2001).
- [7] P. M. Paul *et al.*, *Science* **292**, 1689 (2001).
- [8] M. Hentschel *et al.*, *Nature (London)* **414**, 509 (2001).
- [9] M. Drescher *et al.*, *Nature (London)* **419**, 803 (2002).
- [10] P. Johnsson *et al.*, *Phys. Rev. Lett.* **95**, 013001 (2005).
- [11] R. Wehlitz *et al.*, *Phys. Rev. Lett.* **67**, 3764 (1991).
- [12] G. Tanner, K. Richter, and J. M. Rost, *Rev. Mod. Phys.* **72**, 497 (2000).
- [13] A. S. Kheifets and I. Bray, *J. Phys. B* **36**, L211 (2003).
- [14] J. S. Briggs and V. Schmidt, *J. Phys. B* **33**, R1 (2000).
- [15] A. Y. Istomin, N. L. Manakov, and A. F. Starace, *Phys. Rev. A* **69**, 032713 (2004).
- [16] D. Dundas, K. T. Taylor, J. S. Parker, and E. S. Smyth, *J. Phys. B* **32**, L231 (1999).
- [17] M. S. Pindzola and F. Robicheaux, *Phys. Rev. A* **57**, 318 (1998).
- [18] T. N. Rescigno *et al.*, *Science* **286**, 2474 (1999).
- [19] S. X. Hu, J. Colgan, and L. A. Collins, *J. Phys. B* **38**, L35 (2005); S. X. Hu and L. A. Collins, *Phys. Rev. A* **71**, 062707 (2005).
- [20] B. I. Schneider and L. A. Collins, *J. Non-Cryst. Solids* **351**, 1551 (2005); B. I. Schneider, L. A. Collins and S. X. Hu, *Phys. Rev. E* (to be published).
- [21] A. Knapp *et al.*, *Phys. Rev. Lett.* **89**, 033004 (2002).
- [22] T. F. Gallagher, *Rydberg Atoms* (Cambridge University Press, Cambridge, England, 1994).